P H Y S I C A L   R E V I E W   L E T T E R S

Unconventional Superconductivity with a Sign Reversal in the Order Parameter of LaFeAsO$_{1-x}$F$_x$

I. I. Mazin,[1] D. J. Singh,[2] M. D. Johannes,[1] and M. H. Du[2]

[1]*Code 6393, Naval Research Laboratory, Washington, D.C. 20375, USA*

[2]*Materials Science and Technology Division, Oak Ridge National Laboratory, Oak Ridge, Tennessee 37831-6114, USA*

We argue that the newly discovered superconductivity in a nearly magnetic, Fe-based layered compound is unconventional and mediated by antiferromagnetic spin fluctuations, though different from the usual superexchange and specific to this compound. This resulting state is an example of extended *s*-wave pairing with a sign reversal of the order parameter between different Fermi surface sheets. The main role of doping in this scenario is to lower the density of states and suppress the pair-breaking ferromagnetic fluctuations.

The discovery of superconductivity with $T_c \gtrsim 26$ K [1] in a compound that contains doped Fe^{2+} square lattice sheets raises immediate questions about the nature of the superconducting state and the pairing mechanism. A number of highly unusual properties suggest, even at this early stage, that the superconductivity is not conventional. We argue that not only is it unconventional but that doped LaFeAsO represents the first example of multigap superconductivity with a discontinuous sign change of the order parameter (OP) phase between bands, a state discussed previously (e.g., Refs. [2,3]) but not yet observed in nature.

We suggest that superconductivity here is mediated by spin fluctuations (SFs), as many believe is the case in cuprates, heavy fermion materials, or ruthenates. SFs can induce only a triplet superconducting OP or a singlet one that changes sign over the Fermi surface (FS). The latter condition often, but not always, dictates strong angular anisotropy of the OP (cf. *d* wave). In our scenario, it is satisfied despite full angular isotropy, since the sign changes between the two sets of FSs. Our model is also principally different from conventional *s*-wave superconductivity discovered in MgB$_2$: There the pairing interaction is attractive; in our case it is repulsive (but pairing thanks to the sign reversal). Finally, similar to *d*- or *p*-wave superconductivity, our OP has a nearest-neighbor structure in real space, thus reducing the Coulomb repulsion within the pair.

We begin by arguing against conventional superconductivity. The pure compound LaFeAsO is on the verge of a magnetic instability: It has a very high magnetic susceptibility [1] and is strongly renormalized compared to density functional (DFT) calculations [4]. This renormalization is higher than in any known conventional superconductor, including MgCNi$_3$, where superconductivity is believed to be strongly depressed by spin fluctuations. The susceptibility in the pure compound is large and upon doping with F grows even larger and becomes Curie–Weiss-like. This suggests nearness to a critical point in the pure compound and nontrivial competition between different SFs. Very

strong electron-phonon interactions would be required to overcome the destructive effects of such SFs. We have calculated *ab initio* the electron-phonon spectral function $\alpha^2 F(\omega)$ and coupling λ for the stoichiometric compound [5]. Some moderate coupling exists, mostly to As modes, but the total λ appears to be ~0.2, with $\omega_{\log} \sim$ 250 K ($\omega_{\log}$ is the logarithmically averaged boson frequency of Eliashberg theory), which can in no way explain $T_c \gtrsim 26$ K.

The calculated DFT Fermi surfaces [4] for undoped LaFeAsO consist of two small electron cylinders around the tetragonal *M* point and two hole cylinders, plus a heavy 3D hole pocket around Γ. To study doping effects, we performed full-potential calculations using the WIEN package in the virtual crystal approximation and the Perdew-Burke-Ernzerhof generalized gradient approximation (GGA) functional [6]. The lattice parameters we took from experiment [1] and optimized the internal positions [7]. In Fig. 1, we show the bands near the Fermi level for $x = 0.1$ and the corresponding Fermi surface. As expected, the 3D pocket fills with electron doping (at $x = 0.04$–0.05) and the fermiology radically simplifies, leaving a highly
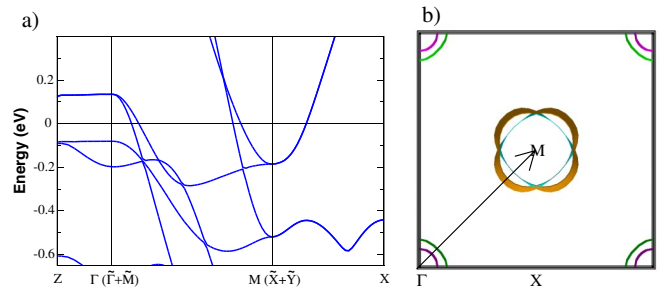

FIG. 1 (color online). (a) Calculated band structure at $x = 0.1$ near the Fermi level. (b) Calculated Fermi surface at 10% doping. Note that the only 3D parts are the far ends of the electron cylinders around *M*. The fully three-dimensional surface present in the undoped compound is suppressed beneath E_F by increased electron count.

2D electronic structure with two heavy hole cylinders and two lighter (and larger) electron cylinders.

This fermiology imposes strong constraints on the superconductivity. In particular, with the exception of phonons, it is hard to identify pairing interactions with a strong k_z dependence. Thus, states with strong variations of the OP along k_z are unlikely. An angular variation of the OP in the xy plane is possible but would require an unrealistically strong **q** dependence of the pairing interaction on the scale of the small Fermi surface size and would also be extremely sensitive to impurities.

On the other hand, the small Fermi surfaces are readily compatible with a pairing state with weak variations of the OP within the sheets but a π phase shift between electron and hole cylinders. Here we show that a SF pairing interaction favoring exactly such a state is present in this material, and we discuss the expected consequent physical properties.

The SF spectrum is unusually rich for this compound and comes from three separate sources. First, the system is relatively close to a Stoner ferromagnetic instability. Second, there is a nearest-neighbor antiferromagnetic (AFM) superexchange [8(d)]. Third, there are nesting-related AFM spin-density-wave-type SFs near wave vectors connecting the electron and hole pockets. The latter appear to be the strongest ones. The corresponding interaction connects the well-separated FS pockets located around Γ and around M. Though repulsive in the singlet channel, these would nevertheless be strongly pairing provided that the OPs on the two sets of the FSs have opposite signs. The main message of our Letter is that this "$s_{\pm}$" superconducting state is both consistent with experimental observations and most favored by SFs in this system.

As opposed to the undoped material [4], we do not find any FM solution for the doped compound, even with the more magnetic GGA functional. This suggests that the main function of doping is to move the system away from a ferromagnetic instability (see, however, Ref. [8]). That the system becomes less magnetic is due to the fact that upon doping the heavy 3D hole pocket near Γ rapidly fills and the total density of states (DOS) drops (by a factor of 2). At a doping level $x = 0.1$, we obtain in the GGA an unrenormalized Pauli susceptibility $\mathrm{Re}\chi_0(\mathbf{q} = 0, \omega = 0) \approx 4 \times 10^{-5}$ emu/mole $[N(0) = 0.64$ states/eV/spin/Fe]. Using 1.1 eV for the Stoner I on Fe, we obtain a renormalized $\chi(0)$ of 0.14×10^{-3} emu/mole, a large renormalization but much smaller than what is needed to explain the experimental value [1]. Note that in the undoped system the calculated susceptibility is larger, and the experimental one smaller, than in the doped one. This suggests that besides FM SFs there are other, more important spin excitations in the system.

The first candidate for these is a superexchange corresponding to the standard simple nearest-neighbor checkerboard antiferromagnetism. Importantly, there is also substantial direct Fe-Fe overlap [4], which leads to an

additional AFM exchange of comparable strength and with the same checkerboard geometry.

Further discussion requires an understanding of the fermiology in clearer terms. The band structure may at first appear intractably complex, but it is in fact relatively simple, involving only three Fe orbitals near the Fermi level. The hole pockets around Γ originate from Fe d_{xz} and d_{yz} bands that are degenerate at Γ and form two nearly perfect concentric cylinders. The electron surfaces are better understood if we recall that the underlying Fe layer forms a square lattice with the period $\tilde{a} = a/\sqrt{2}$ (Fig. 2). The corresponding 2D Brillouin zone (BZ) is twice larger and rotated by 45°. If we could "unfold" the Fermi surface of Fig. 1, we would find the same two hole pockets at $\tilde{\Gamma}$ and *one* electron pocket around the point $\tilde{X}$ in the *large* BZ. The latter is formed by the d_{yz} band (or d_{xz} near $\tilde{Y}$) that starts 180 meV below the Fermi energy, disperses up along $\tilde{X}\tilde{M}$, and is practically flat along $\tilde{X}\tilde{\Gamma}$. This band is hybridized with the d_{xy} band (or $d_{x^2-y^2}$ in the two-Fe cell), which starts from $\tilde{X}$ at an energy of -520 meV and is instead dispersive along $\tilde{X}\tilde{\Gamma}$. Upon hybridization, these two bands yield an oval cylindrical electron pocket, elongated along $\tilde{\Gamma}\tilde{X}$ [9].

Electronic transitions from the hole pockets to the electron pocket should lead to a broad (because the electron pocket is oval rather than circular) peak in the *noninteracting* susceptibility $\chi_0(q, \omega \to 0)$, at $q = (\pi/\tilde{a}, 0)$, while the superexchange interaction $J(q)$ on the square lattice should be peaked at $q = (\pi/\tilde{a}, \pi/\tilde{a})$ (Γ in the downfolded BZ). The renormalized susceptibility $\chi(q) = \chi_0(q)/[1 - J(q)\chi_0(q)]$ then has a rich structure with maxima at $\tilde{\Gamma}$, $\tilde{X}$, and $\tilde{M}$. For the true unit cell with two Fe, both $\tilde{\Gamma}$ and $\tilde{M}$ fold
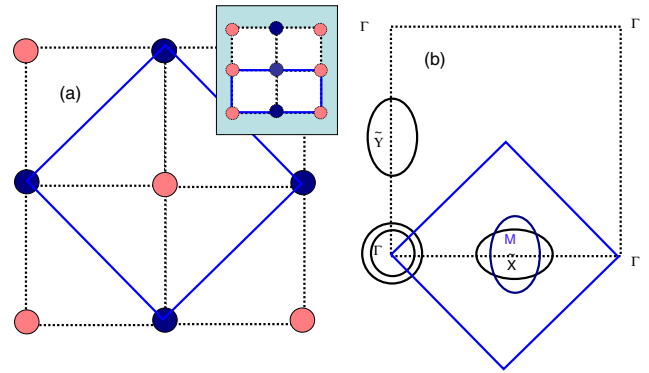

FIG. 2 (color online). Fermi surface formation upon backfolding of the large BZ corresponding to a simple Fe square lattice. (a) Real space: the four small unit cells of the Fe-only sublattice (dashed lines) with the larger solid diamond of actual two-Fe unit cell. Dark and light circles indicate superexchange (checkerboard) ordering. The inset shows the spin-density wave corresponding to $\tilde{X}$ point SFs. (b) Reciprocal space: the dashed black square is the unfolded BZ, the solid blue diamond is the downfolded zone, and the blue ellipse is the electron pocket from the $\tilde{Y}$ point downfolded onto the $\tilde{X}$ point (which is M in the small BZ).

down into the Γ point, while $\tilde{X}$ folds down into the M point.
The corresponding folding of the Fermi surfaces makes the
electron pockets overlap, forming two intersecting surfaces
(Fig. 1). It is important to appreciate from this *gedanken
unfolding* that already on the level of the noninteracting
susceptibility there is a tendency for antiferromagnetic
correlations with a wave vector different from the super-
exchange one.

In Fig. 3, we present the calculated [10] $\chi_0(q, \omega) =$
$\frac{f(\epsilon_k) - f(\epsilon_{k+q})}{\epsilon_k - \epsilon_{k+q} - \omega - i\delta}$ at $\omega \to 0$ and $q_z = \pi/c$ (χ is practically
independent of q_z), The peak at M, derived from interband
transitions, is very broad, as expected, with some structure
around the M point, due to the particular orientation of the
two oval pockets at M and the size difference between the
hole and electron cylinders for finite doping. With minor
modification, this structure is present also in the undoped
compound.

We have also performed magnetic calculations (dis-
cussed in a separate publication) in a supercell correspond-
ing to the superexchange $\mathbf{q} = \tilde{M}$ ($= \Gamma$ in the downfolded
Brillouin zone) and nesting-induced $\mathbf{q} = \tilde{X}$ ($= M$) spin-
density waves. We find, indeed, that the tendency to ferro-
magnetic ordering is suppressed in the doped compound,
while the tendency to nesting-based antiferromagnetism is
present, even leading to an actual instability at the mean
field level. It is worth noting that, while this instability does
not appear in actual superconducting materials, it has been
now found experimentally in the low doping regime [8].

The strong AFM SFs around M favor our proposed $s_\pm$
state. Cases where SF-induced interactions connect two
pockets of the Fermi surfaces, including SFs originating
from electronic transitions between the very same pockets
have been considered in the past [11]. However, they
involved FS pockets related by symmetry, which strongly
restricts the phase relations between them. In our case, the
two sets of pockets are not symmetry related, and nothing
prevents them from assuming arbitrary phases.

For the singlet case, the coupling matrix between the
hole (h) and the electron pockets (e) is negative: $\lambda_{\mathrm{eh}} < 0$.
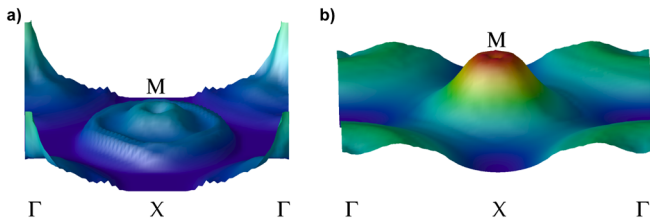The diagonal components emerge from competition be-

FIG. 3 (color online).   The imaginary (a) and the real (b) parts
of the noninteracting susceptibility $\chi_0(q, \omega \to 0)$, in arbitrary
units. Within common approximations $\mathrm{Im}\chi = \mathrm{Im}[\frac{\chi_0}{(1 - J(\mathbf{q})\chi_0(q,w)}]$
is measurable by neutron scattering and $\mathrm{Re}\chi$ controls the pairing
interaction, in the singlet channel proportional to $1/[1 -
J(\mathbf{q})\chi_0(q, 0)]$ (see Ref. [18] for a review). Note that the RPA
enhancement will strengthen both peaks.

tween the attractive phonon-mediated and repulsive SF-
mediated interactions and are, presumably, weak. If $\lambda_{hh}^{\mathrm{ph}}$ is
the average of the phonon-mediated interaction over the
wave vectors $q < 0 < 2k_F^h$, and $\lambda_{hh}^{\mathrm{sf}}$ the same for the SF,
then $\lambda_{hh} = \lambda_{hh}^{\mathrm{ph}} - \lambda_{hh}^{\mathrm{sf}}$. Our calculated electron-phonon
coupling comes mostly from small wave vectors, that is,
$\lambda_{hh}^{\mathrm{ph}} + \lambda_{ee}^{\mathrm{ph}} \approx 0.2$ and $\lambda_{eh}^{\mathrm{ph}} \approx 0$. Phonons, therefore, though
weak, promote the $s_\pm$ state. On the other hand, $\lambda_{hh}^{\mathrm{sf}}$ and $\lambda_{ee}^{\mathrm{sf}}$
come from FM (small-q) SFs and are pair-breaking.
Finally, the superexchange interaction does not affect
λ_{hh}, but the corresponding wave vector $\mathbf{q} = \tilde{\Gamma}\tilde{M}$ connects
the e pockets near $\tilde{X}$ and $\tilde{Y}$, and such fluctuations are also
pair-breaking [8(c)].

The T_c, as usual for a two-gap superconductor [12], is
defined by the maximal eigenvalue of the λ matrix $\lambda_{\mathrm{eff}} =
[\lambda_{hh} + \lambda_{ee} + \sqrt{4\lambda_{eh}\lambda_{he} + (\lambda_{ee} - \lambda_{hh})^2}]/2$, and the OPs
$\Delta_{e,h}$ are defined by the corresponding eigenvector. In our
case, the signs of Δ_h and Δ_e will be opposite, and their
absolute values will be similar since presumably $(\lambda_{ee} -
\lambda_{hh})^2 \ll \lambda_{eh}\lambda_{he}$. This "$s_\pm$" state is analogous to the states
proposed previously for semimetals [13] and bilayer cup-
rates [14].

From the point of view of neutron scattering, the struc-
ture of the peak in χ near M is important, but, for SF-
induced superconductivity, it does not matter at all. A well-
defined spin excitation requires a sharp peak, but the pair-
ing interaction is integrated over all possible q vectors
spanning the two sets of Fermi surfaces so that only the
total weight of the peak is important. Dimensionality is,
however, very important, as 3D coupling supports a long-
range magnetic ordering (competing with superconductiv-
ity). Indeed, experiment shows an abrupt appearance of
superconductivity at $x \approx 0.03$, roughly where the 3D pock-
ets around Γ disappear.

One might envision a triplet state similar to the de-
scribed singlet one, fully gapped, as expected for unitary
2D p-wave states, and with different amplitudes (or signs)
on the two cylinders. The similarity, however, is mislead-
ing. In the triplet channel, SFs induce attraction, but given
the relatively large width of the AF peak (Fig. 3), a large
part of the pairing will be lost as only SF with a wave
vector exactly equal to $(\pi/a, \pi/a)$ will be fully pairing,
and some others will even be pair-breaking. Therefore, in
this scenario where the antiferromagnetic SFs around the
M point provide the primary pairing interaction, we expect
the lowest energy superconducting state to be $s_\pm$. The
structure of the OP in real space can be evaluated using
the lowest Fourier component, compatible with the pro-
posed $s_\pm$ state, namely, $\cos k_x + \cos k_y$ (equivalently,
$\cos\tilde{k}_x \cos\tilde{k}_y$). This corresponds to pairing of electrons that
reside on the nearest neighbors, just as in the d-wave case,
so that the on site Coulomb repulsion is not particularly
destructive for this state.

Finally, we discuss the experimental ramifications of the
$s_\pm$ state. In many aspects they are similar to that of the $s_\pm$

state proposed in Ref. [14] and discussed in some detail in Refs. [14–16]. The thermodynamic and tunneling characteristics are the same as for a conventional two-gap superconductor [12]. The two-gap character, however, may be difficult to resolve, given the dominance of the interband interactions which will render the two gap magnitudes similar. Nonmagnetic small-q intraband (e-e or h-h) scattering as well as the interband spin-flip pairing will not be pair-breaking, but paramagnetic interband scattering will, resulting in a finite DOS below the gap [2], consistent with specific heat measurements [17]. The most interesting feature of the $s_\pm$ state [16] is that the coherence factors for exciting Bogliubov quasiparticles on FS sheets with opposite signs of the OP are reversed compared to conventional coherence factors. We outline a few important consequences of the relatively straightforward application of this concept to experimental probes. First, one expects a qualitative difference between experiments that probe vertical transitions ($\mathbf{q} = 0$) and those that probe transitions with $\mathbf{q}$ close to $\pi/a, \pi/a$. For instance, the spin susceptibility at $\mathbf{q} = 0$ will behave conventionally, i.e., exponentially decay below T_c without any coherence peak, while the susceptibility for $\mathbf{q} \approx \pi/a, \pi/a$ will have a coherence peak that should be detectable by neutron scattering as an enhancement below T_c [16]. AFM SFs near $\pi/a, \pi/a$ dominate in the doped material, and so the usual coherence peak in the NMR relaxation rate, which averages equally over all wave vectors, is expected to disappear or be strongly reduced. It was shown in Ref. [15] that Josephson currents from FSs with different signs of the OP interfere destructively, and the net phase corresponds to the sign of the FS with the higher normal conductance. In the constant relaxation time approximation, both in-plane and out-of-plane conductivities are dominated by the electron pockets. This is unfortunate, since there would otherwise be a π phase shift between the ab and c tunneling, and corner-junction experiments could be used, as in high-T_c cuprates.

In summary, we argue that the fermiology found in doped LaAsFeO gives rise to strong but broad antiferromagnetic spin fluctuations near the M point in the Brillouin zone, while the tendency to magnetism existing at zero doping is suppressed. These fluctuations, while too broad to induce a magnetic instability, are instrumental in creating a superconducting state with OPs of opposite signs on the electron and hole pockets.

[1] Y. Kamihara *et al.*, J. Am. Chem. Soc. **130**, 3296 (2008)..

[2] A. A. Golubov and I. I. Mazin, Phys. Rev. B **55**, 15 146 (1997).

[3] D. F. Agterberg, V. Barzykin, and L. P. Gor'kov, Phys. Rev. B **60**, 14 868 (1999).

[4] D. J. Singh and M. H. Du, Phys. Rev. Lett. **100**, 237003 (2008).

[5] We used linear response theory with ultrasoft pseudopotentials as implemented within the QUANTUM ESPRESSO package by S. Baroni *et al.*, http://www.pwscf.org/. We used a zone sampling of 1377 inequivalent $\mathbf{k}$ points, a $4 \times 4 \times 2$ phonon mesh, and a plane wave cutoff of 50 Ry.

[6] J. P. Perdew, S. Burke, and M. Ernzerhof, Phys. Rev. Lett. **77**, 3865 (1996).

[7] The optimized positions actually depend slightly on doping. For $x = 0.1$, in GGA, they are $z_{La} = 0.148$ and $z_{As} = 0.638$.

[8] After this manuscript was submitted for publication, several dozen relevant preprints have been posted, in particular, (a) experimental verification of the spin-density wave (SDW) state predicted here (inset in Fig. 2), at $x \lesssim 0.05$ (M. A. McGuire *et al.*, arXiv:0804.0796); (b) while we calculated the SDW stripe ordered phase at $x = 0.1$, Dong Sun *et al.*, arXiv:0803.2883 have subsequently shown that, contrary to our initial conjecture, at zero doping this instability is even stronger; (c) K. Kuroki *et al.*, arXiv:0803.3325 have studied the SF-induced superconductivity in LaFeAsO adding the RPA renormalization to our model and found that the $s_\pm$ state has the lowest energy as long as the hole pockets are present (otherwise, a nodeless d-wave state is the most stable one); and (d) T. Yildirim, arXiv:0804.2252 has pointed out that the next-nearest-neighbor superexchange in this system is of the same order as the nearest-neighbor superexchange, adding a fourth nontrivial magnetic interaction to those we considered. These and other recent results support our main proposition that the role of doping is to drive the system away from a magnetic instability, though we misidentified the offending instability as ferromagnetic.

[9] We thank P. A. Lee for pointing out an erroneous transmutation of $\tilde{X}$ and $\tilde{Y}$ in our original description.

[10] We used a three-dimensional grid of $\approx 75\,000$ k and q points with a temperature smearing of 1 mRy and the constant matrix element approximation.

[11] M. D. Johannes, I. I. Mazin, D. J. Singh, and D. A. Papaconstantopoulos, Phys. Rev. Lett. **93**, 097005 (2004); K. Voelker and M. Sigrist, arXiv:cond-mat/0208367.

[12] I. I. Mazin and V. P. Antropov, Physica (Amsterdam) **385C**, 49 (2003).

[13] A. G. Aronov and E. B. Sonin, Zh. Eksp. Teor. Fiz. **63**, 1059 (1972) [Sov. Phys. JETP **36**, 556 (1973)].

[14] A. I. Liechtenstein, I. I. Mazin, and O. K. Andersen, Phys. Rev. Lett. **74**, 2303 (1995).

[15] I. I. Mazin, A. A. Golubov, and A. D. Zaikin, Phys. Rev. Lett. **75**, 2574 (1995).

[16] I. I. Mazin and V. Yakovenko, Phys. Rev. Lett. **75**, 4134 (1995).

[17] G. Mu, X. Zhu, L. Fang, L. Shan, C. Ren, and H. H. Wen, arXiv:0803.0928.

[18] T. Moria and K. Ueda, Rep. Prog. Phys. **66**, 1299 (2003).